

# Vapor–Liquid Equilibrium Data for the Ethylene + Hexane System

Istvan Nagy,<sup>†</sup> Ryan A. Krenz,<sup>‡</sup> Robert A. Heidemann,<sup>‡</sup> and Theo W. de Loos<sup>\*,†</sup>

Delft University of Technology, Department of Chemical Technology, Physical Chemistry and Molecular Thermodynamics, Julianalaan 136, 2628 BL Delft, The Netherlands, and University of Calgary, Department of Chemical and Petroleum Engineering, 2500 University Drive NW, Calgary, Alberta T2N 1N4, Canada

Vapor–liquid equilibrium data have been measured for the ethylene + hexane system at temperatures of (390 to 510) K and pressures up to 10 MPa. The bubble and dew point pressures of ethylene + hexane samples with fixed compositions were measured using the Cailletet apparatus. The critical points of ethylene + hexane mixtures were also measured experimentally. The experimental data were correlated with the modified Sanchez–Lacombe (MSL) equation of state. The experimental data are also compared with the predictions of the Peng–Robinson (PR) and Soave–Redlich–Kwong (SRK) equations of state using the binary interaction parameter obtained in the MSL correlation. The three equations of state produce comparable qualitative representations of the experimental phase boundaries.

## Introduction

High-pressure vapor–liquid equilibrium data are required for process design and control. Vapor–liquid equilibrium data have previously been measured for the system of ethylene + hexane.<sup>1–6</sup> Most of the available experimental data are at low ethylene compositions, at temperatures below 390 K, and/or only the critical points. The purpose of this work is to obtain experimental bubble and dew point data for the ethylene + hexane system at temperatures of (390 to 510) K and pressures up to 10 MPa. The ranges of temperature and pressure have application in the solution polymerization process used to produce polyethylene industrially. The phase behavior of the ternary system polymer + solvent + ethylene and its binary subsystems should be known for the design of this process because hydrocarbons are used as solvents.

The experimental data are modeled with an equation of state for polymer solutions: the modified Sanchez–Lacombe (MSL) equation of state with one adjustable binary interaction parameter. The same value of the binary interaction parameter is also used to calculate a phase boundary using both the Peng–Robinson (PR) and Soave–Redlich–Kwong (SRK) equations of state.

## Experimental Section

**Materials and Sample Preparation.** Ethylene (C<sub>2</sub>H<sub>4</sub>, certified GC purity >99.95%) was obtained from AGA Gas BV (product number AGA 3.5, The Netherlands). Hexane (C<sub>6</sub>H<sub>14</sub>, certified GC purity >99.5%) was obtained from Fluka Chemika (product number 52765, The Netherlands). Approximately (60 to 80) mg of liquid hexane was injected into the base of the Cailletet tube (capillary Pyrex glass tube) using an uncalibrated syringe. The mass of hexane was determined using a microbalance whose precision is estimated to be 0.05 mg. Immersing the base of the glass tube in liquid nitrogen to freeze the hexane and then applying a vacuum degases the sample. The degassing

procedure is usually repeated between three and five times to ensure that the volatile components are completely removed. The hexane sample is frozen and the tube is evacuated before ethylene gas is dosed into a glass bulb.

Mercury is used to seal the ethylene in a glass bulb with a calibrated volume. The pressure and temperature are recorded at this point. The mass of ethylene was determined using the generalized virial expression<sup>7</sup> proposed by Pitzer and co-workers. Ethylene was nearly an ideal gas under filling conditions because the calculated compressibility factors were between 0.9998 and 0.9999. The mercury acts as a piston forcing the ethylene into the Cailletet tube and sealing the sample at the same time. The mixture of ethylene + hexane was prepared with an uncertainty in the mole fraction of less than  $\pm 0.0003$ .

**Experimental Procedure.** The experiments were carried out using the Cailletet apparatus that was described in detail by de Loos et al.<sup>8</sup> The Cailletet tube containing the sample of fixed composition was immersed in a bath of circulating silicon oil to maintain the temperature to within 0.03 K. Experiments were carried out at constant temperature starting in the two-phase region. The pressure was increased in small increments until one of the phases just disappears. Once the phase disappears, the pressure is decreased by the same increment to confirm that the phase reappears. If the incipient phase descends when formed, it is characteristic of dew point behavior; otherwise, if it ascends, it is characteristic of bubble point behavior. The critical temperature of the mixture was measured by determining the temperature interval in which the observed incipient phase changes from bubble point to dew point behavior.

The temperature was measured using a platinum resistance thermometer (uncertainty  $\pm 0.01$  K). The pressure was measured using a dead weight pressure gauge (uncertainty  $\pm 0.002$  MPa at pressures below 5 MPa and  $\pm 0.01$  MPa at pressures equal to and above 5 MPa). The total uncertainty in the temperature is estimated to be  $\pm 0.03$  K as derived from the accuracy of the thermometer, its position in the thermostat fluid relative to the sample, and variances due to the circulation of the thermostat fluid. The total uncertainty in the pressure is  $\pm 0.003$  MPa at pres-

\* Corresponding author. E-mail: t.w.delooos@tnw.tudelft.nl. Tel: +31-15-278 8478. Fax: +31-15-278 8713.

<sup>†</sup> Delft University of Technology.

<sup>‡</sup> University of Calgary.

**Table 1. Experimental Bubble (BP) and Dew (DP) Point Data for Ethylene (1) + Hexane (2)<sup>a</sup>**

| $x_1 = 0.0994$ |       |      | $x_1 = 0.2002$ |       |      | $x_1 = 0.3006$ |       |      |
|----------------|-------|------|----------------|-------|------|----------------|-------|------|
| T/K            | P/MPa | type | T/K            | P/MPa | type | T/K            | P/MPa | type |
| 391.36         | 1.509 | BP   | 390.99         | 2.746 | BP   | 390.75         | 4.092 | BP   |
| 396.27         | 1.584 | BP   | 396.08         | 2.856 | BP   | 395.93         | 4.237 | BP   |
| 401.05         | 1.659 | BP   | 401.12         | 2.961 | BP   | 400.60         | 4.372 | BP   |
| 406.13         | 1.744 | BP   | 405.95         | 3.076 | BP   | 405.66         | 4.517 | BP   |
| 411.04         | 1.824 | BP   | 410.91         | 3.201 | BP   | 410.61         | 4.652 | BP   |
| 415.98         | 1.919 | BP   | 415.83         | 3.306 | BP   | 415.58         | 4.787 | BP   |
| 420.89         | 2.009 | BP   | 420.74         | 3.416 | BP   | 420.36         | 4.927 | BP   |
| 425.84         | 2.104 | BP   | 425.70         | 3.536 | BP   | 425.44         | 5.057 | BP   |
| 430.77         | 2.209 | BP   | 430.74         | 3.656 | BP   | 430.39         | 5.192 | BP   |
| 435.67         | 2.309 | BP   | 435.69         | 3.781 | BP   | 435.36         | 5.312 | BP   |
| 440.65         | 2.414 | BP   | 440.72         | 3.901 | BP   | 440.49         | 5.437 | BP   |
| 445.66         | 2.529 | BP   | 445.91         | 4.031 | BP   | 445.31         | 5.542 | BP   |
| 450.62         | 2.649 | BP   | 450.74         | 4.151 | BP   | 450.28         | 5.652 | BP   |
| 455.59         | 2.769 | BP   | 455.69         | 4.271 | BP   | 455.26         | 5.737 | BP   |
| 460.48         | 2.894 | BP   | 460.59         | 4.386 | BP   | 460.28         | 5.807 | BP   |
| 465.43         | 3.024 | BP   | 465.62         | 4.501 | BP   | 465.16         | 5.847 | BP   |
| 470.48         | 3.159 | BP   | 470.54         | 4.611 | BP   | 470.12         | 5.827 | BP   |
| 475.48         | 3.289 | BP   | 475.41         | 4.701 | BP   | 474.98         | 5.707 | BP   |
| 480.36         | 3.429 | BP   | 480.37         | 4.766 | BP   | 479.99         | 5.417 | DP   |
| 485.34         | 3.564 | BP   | 485.33         | 4.781 | BP   | 484.83         | 4.887 | DP   |
| 490.29         | 3.694 | BP   | 491.31         | 4.516 | DP   |                |       |      |
| 495.25         | 3.804 | BP   |                |       |      |                |       |      |

| $x_1 = 0.4002$ |       |      | $x_1 = 0.4998$ |       |      | $x_1 = 0.6006$ |       |      |
|----------------|-------|------|----------------|-------|------|----------------|-------|------|
| T/K            | P/MPa | type | T/K            | P/MPa | type | T/K            | P/MPa | type |
| 391.04         | 5.434 | BP   | 391.18         | 6.854 | BP   | 391.03         | 8.299 | BP   |
| 396.08         | 5.589 | BP   | 396.13         | 7.039 | BP   | 395.96         | 8.449 | BP   |
| 401.00         | 5.754 | BP   | 401.10         | 7.204 | BP   | 400.85         | 8.559 | BP   |
| 405.85         | 5.914 | BP   | 405.95         | 7.359 | BP   | 405.88         | 8.644 | BP   |
| 410.85         | 6.064 | BP   | 411.05         | 7.504 | BP   | 410.95         | 8.674 | BP   |
| 415.84         | 6.214 | BP   | 415.98         | 7.629 | BP   | 415.81         | 8.649 | BP   |
| 420.76         | 6.349 | BP   | 420.83         | 7.724 | BP   | 420.68         | 8.564 | BP   |
| 425.73         | 6.479 | BP   | 425.97         | 7.794 | BP   | 425.31         | 8.484 | BP   |
| 430.62         | 6.594 | BP   | 431.01         | 7.829 | BP   | 430.71         | 8.229 | DP   |
| 435.60         | 6.699 | BP   | 435.78         | 7.791 | BP   | 435.58         | 7.994 | DP   |
| 440.59         | 6.784 | BP   | 440.78         | 7.714 | BP   | 440.56         | 7.699 | DP   |
| 445.54         | 6.829 | BP   | 446.00         | 7.534 | BP   | 445.51         | 7.264 | DP   |
| 450.41         | 6.849 | BP   | 450.76         | 7.319 | DP   |                |       |      |
| 455.35         | 6.809 | BP   | 455.65         | 6.989 | DP   |                |       |      |
| 460.24         | 6.694 | BP   | 460.56         | 6.564 | DP   |                |       |      |
| 465.22         | 6.454 | BP   |                |       |      |                |       |      |
| 470.26         | 6.139 | DP   |                |       |      |                |       |      |
| 475.06         | 5.629 | DP   |                |       |      |                |       |      |

| $x_1 = 0.7007$ |       |      |
|----------------|-------|------|
| T/K            | P/MPa | type |
| 390.90         | 9.090 | BP   |
| 395.79         | 9.080 | BP   |
| 400.68         | 9.050 | BP   |
| 405.74         | 8.950 | DP   |
| 410.67         | 8.840 | DP   |
| 415.61         | 8.670 | DP   |
| 420.61         | 8.420 | DP   |
| 425.46         | 8.050 | DP   |

<sup>a</sup> Data are ethylene mole fraction  $x_1$ , temperature  $T$ , and pressure  $P$ .

tures below 5 MPa and  $\pm 0.02$  MPa at pressures above 5 MPa. The total uncertainty in pressure is most strongly controlled by the accuracy of the dead weight pressure gauge. At a given composition, the accuracy of the measured critical temperature is  $\pm 0.1$  K, and that of the critical pressure is  $\pm 0.03$  MPa.

## Results

The experimental bubble and dew point measurements are given in Table 1, and the critical point measurements are given in Table 2. Only the upper portion of the ethylene + hexane phase boundary was measured. Isoleths are lines of constant composition and are presented in the  $P$ ,  $T$  graphs shown in Figures 1 and 2. The critical points of

**Table 2. Experimental Critical Point Data for Ethylene (1) + Hexane (2)<sup>a</sup>**

| $x_{1,c}$ | $T_c$ /K | $P_c$ /MPa |
|-----------|----------|------------|
| 0.2002    | 491.28   | 4.519      |
| 0.3006    | 479.65   | 5.437      |
| 0.4002    | 467.21   | 6.336      |
| 0.4998    | 449.90   | 7.346      |
| 0.6006    | 428.18   | 8.321      |
| 0.7007    | 402.32   | 9.021      |

<sup>a</sup> Data are critical ethylene mole fraction  $x_{1,c}$ , critical temperature  $T_c$ , and critical pressure  $P_c$ .

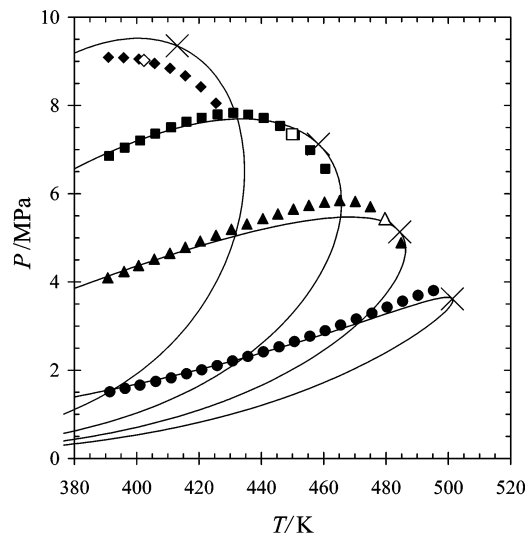


**Figure 1.** Vapor-liquid equilibrium data for the ethylene (1) + hexane (2) system. Filled symbols are bubble and dew points, empty symbols are critical points, curves are phase boundaries, and crosses ( $\times$ ) are critical points calculated using the MSL-EoS and  $k_{ij} = 2.905 \times 10^{-2}$ . Ethylene mole fraction:  $\bullet$ ,  $x_1 = 0.0994$ ;  $\blacktriangle$ ,  $x_1 = 0.3006$ ;  $\blacksquare$ ,  $x_1 = 0.4998$ ;  $\blacklozenge$ ,  $x_1 = 0.7007$ .

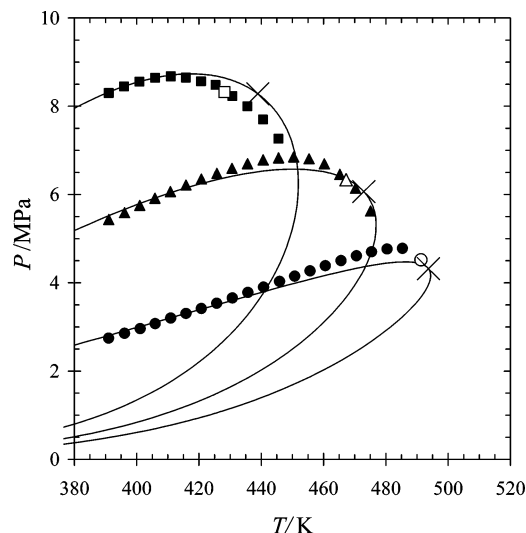


**Figure 2.** Vapor-liquid equilibrium data for the ethylene (1) + hexane (2) system. Filled symbols are bubble and dew points, empty symbols are critical points, curves are phase boundaries, and crosses ( $\times$ ) are critical points calculated using the MSL-EoS and  $k_{ij} = 2.905 \times 10^{-2}$ . Ethylene mole fraction:  $\bullet$ ,  $x_1 = 0.2002$ ;  $\blacktriangle$ ,  $x_1 = 0.4002$ ;  $\blacksquare$ ,  $x_1 = 0.6006$ .

the ethylene + hexane mixtures are located at higher temperatures than the maximum pressure of a mixture with given composition. The critical temperature  $T_c$  and critical pressure  $P_c$  as a function of the ethylene mole fraction  $x_1$  are presented in Figures 3 and 4, respectively.

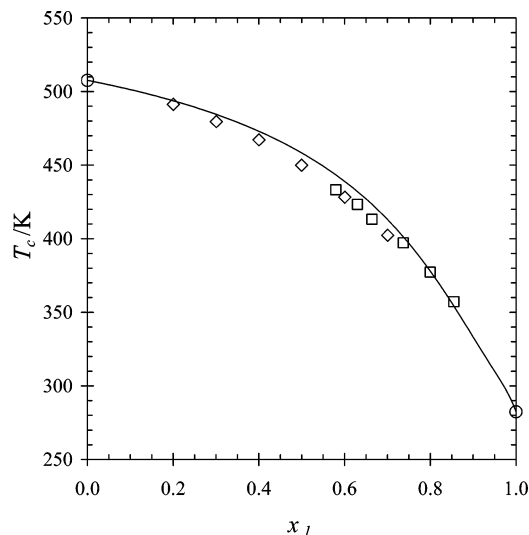


**Figure 3.** Critical temperature  $T_c$  versus ethylene mole fraction  $x_1$  for the ethylene (1) + hexane (2) system. Empty symbols are experimental data, and curves are calculated using the MSL-EoS and  $k_{ij} = 2.905 \times 10^{-2}$ . Sources of data:  $\circ$ , Poling et al.;<sup>14</sup>  $\square$ , Rätzsch and Söll;<sup>4</sup>  $\diamond$ , this work.

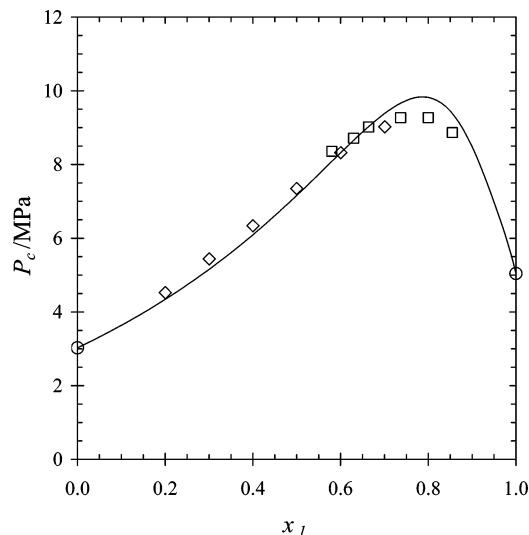


**Figure 4.** Critical pressure  $P_c$  versus ethylene mole fraction  $x_1$  for the ethylene (1) + hexane (2) system. Empty symbols are experimental data, and curves are calculated using the MSL-EoS and  $k_{ij} = 2.905 \times 10^{-2}$ . Sources of data:  $\circ$ , Poling et al.;<sup>14</sup>  $\square$ , Rätzsch and Söll;<sup>4</sup>  $\diamond$ , this work.

The critical point data measured by Rätzsch and Söll<sup>4</sup> are compared to those of the present work in Figures 3 and 4. The two sets of experimental data are in relatively good agreement over the entire range.

The modified Sanchez–Lacombe equation of state (MSL-EoS)<sup>9</sup> was used to perform the calculations using a parametrization that obtains the pure component parameters from the critical temperature, pressure, and acentric factor.<sup>10</sup> The MSL equation and correlation procedure are presented elsewhere in more detail.<sup>11</sup> The Peng–Robinson (PR)<sup>12</sup> and Soave–Redlich–Kwong (SRK)<sup>13</sup> equations of state are also used to model the experimental data.

A classic quadratic mixing rule is used for the energetic parameter  $a$  in all three equations of state

$$a = \sum_i \sum_j x_i x_j a_{ij} (1 - k_{ij}) \quad (1)$$

**Table 3. Solvent Properties<sup>14 a</sup>**

| solvent  | $M/\text{g}\cdot\text{mol}^{-1}$ | $\omega$ ( $T_r = 0.7$ ) | $T_c/\text{K}$ | $P_c/\text{MPa}$ |
|----------|----------------------------------|--------------------------|----------------|------------------|
| ethylene | 28.054                           | 0.087                    | 282.34         | 5.041            |
| hexane   | 86.177                           | 0.300                    | 507.60         | 3.025            |

<sup>a</sup> Molar mass  $M$ , acentric factor  $\omega$ , critical temperature  $T_c$ , and critical pressure  $P_c$ .

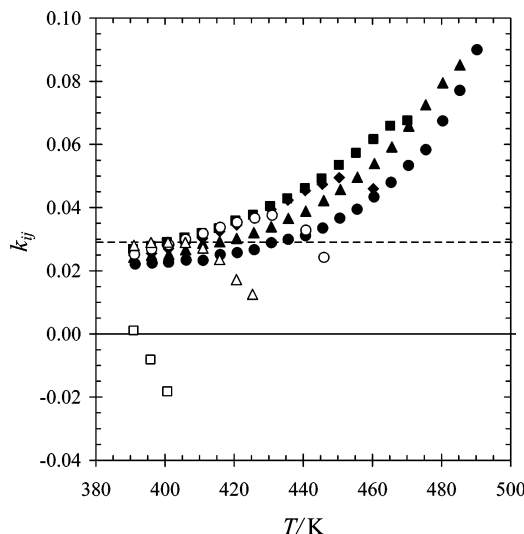


**Figure 5.** Ethylene (1) + hexane (2) binary interaction parameters  $k_{ij}$  required for the MSL-EoS to match each experimental data point. The dashed line is  $k_{ij} = 2.905 \times 10^{-2}$ . Ethylene mole fraction:  $\bullet$ ,  $x_1 = 0.0994$ ;  $\blacktriangle$ ,  $x_1 = 0.2002$ ;  $\blacksquare$ ,  $x_1 = 0.3006$ ;  $\blacklozenge$ ,  $x_1 = 0.4002$ ;  $\circ$ ,  $x_1 = 0.4998$ ;  $\triangle$ ,  $x_1 = 0.6006$ ;  $\square$ ,  $x_1 = 0.7007$ .

where  $x_i$  and  $x_j$  are the molar compositions,  $a_{ij}$  is the cross parameter, and  $k_{ij}$  is the binary interaction parameter. The properties of ethylene and hexane taken from ref 14 are listed in Table 3.

The binary interaction parameters required for the MSL-EoS to match each experimental data point are shown in Figure 5. The binary interaction parameters required are not significantly dependent on the composition of the mixture. There is a definite curvature with respect to temperature in the binary interaction parameters. The binary interaction parameters as a function of temperature at different compositions have similar curvatures except near the critical point of each composition.

The sensitivity of the phase boundary to changes in the binary interaction parameters is more important. The objective function  $f_{xPT}$  used to obtain the MSL binary interaction parameter in this work is

$$f_{xPT} = \frac{1}{N_{xPT}} \left[ \sum_{k=1}^{N_{xPT}} |T_{(k)} - T_{(k)}^o| \right] + \frac{(N_{xPT}^o - N_{xPT})}{N_{xPT}} \times 100 \quad (2)$$

$N_{xPT}^o$  is the total number of experimental data points, whereas  $N_{xPT}$  is the total number of converged points in the calculations. The subscript  $(k)$  refers to an experimental data point where the calculated temperature  $T_{(k)}$  is compared to the experimental temperature  $T_{(k)}^o$ . It is more typical to report the absolute average deviation (AAD) in bubble and dew point temperatures for the converged points.

$$\text{AAD } T = \frac{1}{N_{xPT}} \left[ \sum_{k=1}^{N_{xPT}} |T_{(k)} - T_{(k)}^o| \right] \quad (3)$$

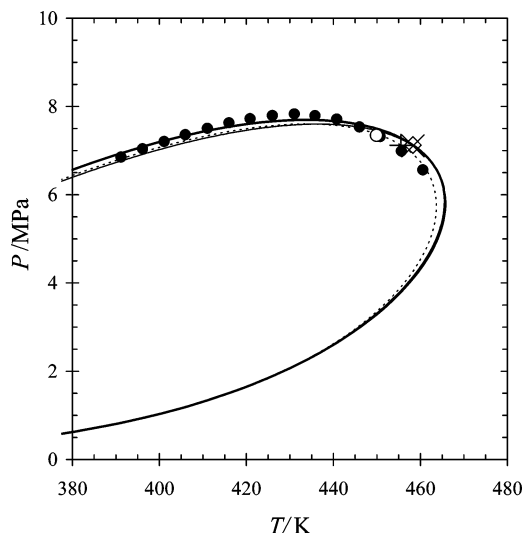


**Figure 6.** Phase boundary isopleth for a 0.4998 ethylene (1) + hexane (2) mixture. Experimental data: ●, bubble or dew point; ○, critical point. Curves are phase boundaries, and symbols are critical points calculated using different equations of state with  $k_{ij} = 2.905 \times 10^{-2}$ . — and ◇, MSL; - - - and +, PR; - · - and ×, SRK.

The MSL binary interaction parameter was  $k_{ij} = 2.905 \times 10^{-2}$  based on 79 of 116 points converged. The absolute average deviation in temperature was AAD  $T = 4.88$  K (1.15 %). Using a temperature-independent binary interaction parameter does not cause a significant decrease in accuracy over the entire range of temperature.

The MSL-EoS provides a qualitative representation of the experimental data presented in Figures 1 through 4 with a single binary interaction parameter. In Figures 1 and 2, the model deviates most from the experimental data at a given composition near the critical point. The MSL equation provides a fairly good representation of the critical temperature of an ethylene + hexane system as shown in Figure 3. Figure 4 demonstrates that the critical pressure of an ethylene + hexane system is only qualitatively represented by the MSL equation of state because the equation overpredicts the maximum critical pressure by approximately 0.6 MPa.

Phase boundary calculations performed with the PR and SRK equations of state that use the MSL binary interaction

parameter are shown in Figure 6. There is a marginal difference in the accuracy of the calculations using the three equations of state. The critical point calculated using the PR equation is closer to the experimental critical point. The critical points are nearly the same using the same binary interaction parameter for the MSL and SRK equations. The three equations of state produce comparable-qualitative representations of the experimental phase boundaries.

#### Literature Cited

- (1) McDaniel, A. S. The Absorption of Hydrocarbon Gases by Non-Aqueous Liquids. *J. Phys. Chem.* **1911**, *15*, 587–610.
- (2) Zhuze, T. P.; Zhurba, A. S. Solubilities of Ethylene in Hexane, Cyclohexane, and Benzene under Pressure. *Bull. Acad. Sci. USSR, Div. Chem. Sci.* **1960**, *2*, 335–337.
- (3) Waters, J. A.; Mortimer, G. A.; Clements, H. E. Solubility of Some Light Hydrocarbons and Hydrogen in Some Organic Solvents. *J. Chem. Eng. Data* **1970**, *15*, 174–176.
- (4) Rätzsch, M.; Söll, W. Critical Liquid–Vapor Phenomena of Binary Systems with Ethylene. *Z. Phys. Chem. (Leipzig)* **1975**, *256*, 815–828.
- (5) Sahgal, A.; La, H. M.; Hayduk, W. Solubility of Ethylene in Several Polar and Non-Polar Solvents. *Can. J. Chem. Eng.* **1978**, *56*, 354–357.
- (6) Heller, D.; Bilda, D. Ethen-Löslichkeit in Ausgewählten Kohlenwasserstoffen. *Chem.-Ing.-Tech.* **1990**, *62*, 928–930.
- (7) Smith, J. M.; van Ness, H. C.; Abbott, M. M. *Introduction to Chemical Engineering Thermodynamics*, 5th ed.; McGraw-Hill: New York, 1996.
- (8) de Loos, Th. W.; van der Kooij, H. J.; Ott, P. L. Vapor–Liquid Critical Curve of the System Ethane + 2-Methylpropane. *J. Chem. Eng. Data* **1986**, *31*, 166–168.
- (9) Neau, E. A Consistent Method for Phase Equilibrium Calculation Using the Sanchez-Lacombe Lattice-Fluid Equation-of-State. *Fluid Phase Equilib.* **2002**, *203*, 133–140.
- (10) Gauter, K.; Heidemann, R. A. A Proposal for Parametrizing the Sanchez–Lacombe Equation of State. *Ind. Eng. Chem. Res.* **2000**, *39*, 1115–1117.
- (11) Krenz, R. A. Ph.D. Dissertation, University of Calgary, Calgary, Canada, 2005.
- (12) Peng, D.-Y.; Robinson, D. B. A New Two-Constant Equation of State. *Ind. Eng. Chem. Fundam.* **1976**, *15*, 59–64.
- (13) Soave, G. Equilibrium Constants from a Modified Redlich-Kwong Equation of State. *Chem. Eng. Sci.* **1972**, *27*, 1197–1203.
- (14) Poling, B. E.; Prausnitz, J. M.; O’Connell, J. P. *The Properties of Gases and Liquids*, 5th ed.; McGraw-Hill: New York, 2000.

Received for review March 24, 2005. Accepted May 11, 2005. The funding for the Canadian portion of this research was provided by the Natural Sciences and Engineering Research Council (NSERC) of Canada and Nova Research and Technology Corporation (Calgary, Alberta).

JE050120S